

Finite-Span Effect on Vortex-Induced Vibration Simulations

Xingeng Wu¹, Anupam Sharma^{2,*}

Department of Aerospace Engineering, Iowa State University, Ames, Iowa, 50011

Abstract

The effects of spanwise periodic boundary conditions to simulate vortex induced vibration (VIV) of finite-span cylinders are investigated. Flow over four elastically-mounted rigid circular cylinder models of varying span lengths are studied using detached eddy simulations. Spectra of integrated transverse loading and spanwise coherence of sectional force coefficient are analyzed to explain the observed differences. Aspect ratio of ten is found to be sufficient to accurately simulate VIV.

1. Introduction

Vortex-induced vibrations (VIV) are commonly observed in bridge decks, cables, power conductors, risers in oil rigs, etc. The Kármán vortex shedding in the wake of the cylinder produces periodic forcing on the cylinder. In certain conditions the vortex-shedding frequency synchronizes (“lock-in”) with the natural frequency of the system which results in high-amplitude oscillations limited only by the system damping. Experimental investigations of VIV are typically performed with finite-span cylinders with aspect ratios greater than 10 to minimize “end effects” (*cite*), where end-effects refer to effects due to three-dimensional flow at span ends. End plates have been used in experiments (*cite*), which reduce but not completely eliminate the end effects as horse-shoe vortices develop at the intersection of the cylinder and the end plates.

This problem is avoided in simulations by using periodic boundaries in the span direction. While the periodic boundaries imply an infinitely-long cylinder, the finite size of the computational domain in the span direction imposes artificial periodicity in the flow. If spanwise variations are present in the flow and the length scale of these variations is larger than the simulated span, then span periodicity will likely yield incorrect results. For a turbulent flow (stochastic system), this length scale can be measured using two-point correlations; in particular, spanwise coherence. Magnitude-squared coherence is defined as $\gamma^2(\Delta z, f) = \langle |S_{xy}(f)|^2 \rangle / (\langle S_{xx}(f) \rangle \langle S_{yy}(f) \rangle)$, where $S_{xy}(f)$ denotes cross-spectral density of the desired quantity (e.g., sectional force) at points \mathbf{x} and \mathbf{y} separated by a distance Δz (along the span). $S_{xx}(f)$ and $S_{yy}(f)$ are auto-spectral densities at \mathbf{x} and \mathbf{y} respectively, and angle brackets denote ensemble averaging.

*Corresponding author

Email address: sharma@iastate.edu (Anupam Sharma)

¹Graduate Student

²Associate Professor, Iowa State University

Figure 1 presents contours of $\gamma^2(\Delta z, \omega)$ of sectional transverse force for a static circular cylinder (aspect ratio, $L/D=20$) simulation. Nondimensional frequency, $k = f D/V_\infty$ is used to plot coherence. Spanwise coherence is small everywhere except at the Kármán vortex-shedding frequency (f_v), which is given by the Strouhal number, $St = f_v D/V_\infty$ (~ 0.2).

In this paper, we investigate the effect of span periodicity when simulating a circular cylinder experiencing VIV. While the effect of aspect ratio (span length to diameter ratio, L/D) have been investigated in VIV experiments (*cite*), such an investigation is lacking for simulations. (* provide a very brief summary of study on aspect-ratio-effects for flow over a cylinder *) We present detached eddy simulation (DES) results of four models with $L/D = 1, 2, 5$, and 10 . Displacement amplitude, oscillation frequency, lift spectra and spanwise coherence are analyzed to study the effect of span periodicity.

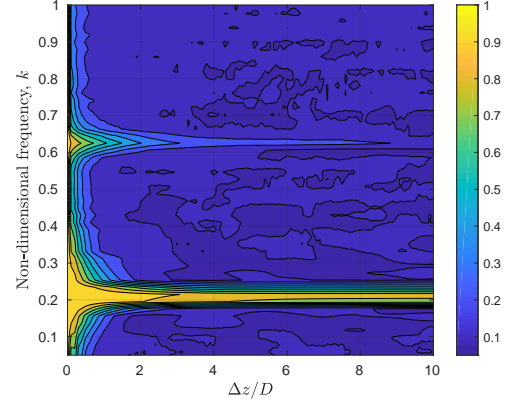


Figure 1: $\gamma^2(\Delta z, f)$ for a static cylinder

2. Computational Methodology and Verification

A coupled fluid-solid dynamics solver is used to simulate an elastically-mounted rigid circular cylinder experiencing VIV. The k - ω detached eddy simulation (DES) technique [1] is used to model the flow and a forced single-degree of freedom mass-spring-damper system is solved to model the dynamics of the cylinder. The details of the numerical methodology are described in Wu *et al.* [2].

Figure 2 (a) shows a schematic of the simulation setup and a comparison with measured data from Ref. [3] for a low mass-damping cylinder undergoing VIV. The following nondimensional numbers are matched between the experiment and the simulations: mass ratio, $m^* = 2.6$, mechanical damping ratio, $\zeta = 0.001$, and reduced velocity, $V_R = V_\infty/(f_N D)$, where f_N is the natural frequency of the system (mounted cylinder). The flow Reynolds number based on the cylinder diameter, $Re_D = 2 \times 10^4$. The simulations accurately predict the displacement amplitude and the vortex shedding frequency of the cylinder (see Fig. 2) over a wide range of V_R which includes the four branches identified in Ref. [3]: *Initial Excitation*, *Upper*, *Lower*, and *Desynchronization*. Of particular interest is the “lock-in” phenomenon which occurs in the *Upper* and *Lower* branches where the chances of structural damage are highest.

3. Effect of Aspect Ratio

Four cylinder models with aspect ratio, $L/D = 1, 2, 5$, and 10 are evaluated using DES with periodic span boundaries. For each configuration, seven values of reduced velocity V_R ($= 2, 3, 4, 5, 5.9, 7, 8$) are evaluated; this wide range of V_R covers the *Initial Excitation*, *Upper*, and *Lower* branches. Figure 3 compares the predicted scaled mean amplitude (\bar{A}/D) and the normalized oscillation frequency (f_v/f_N) for the different models. The convergence of the results for models with $L/D = 5$ and 10 shows that span length of $10 \times D$ is adequate

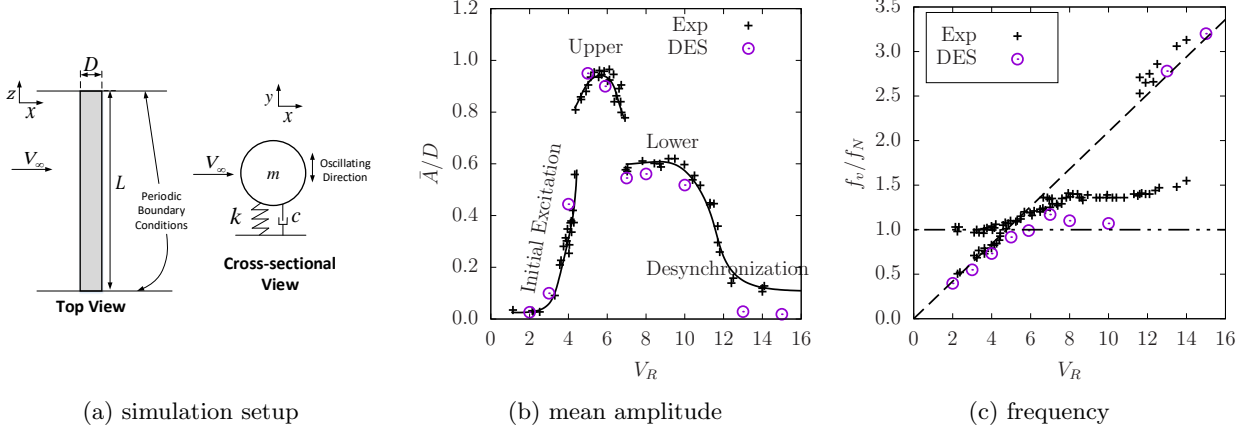


Figure 2: Verification of the DES approach to predict VIV: (a) a schematic showing the simulation setup, (b) mean nondimensional displacement amplitude (\bar{A}/D), and (c) normalized oscillation frequency (f_v/f_N). Measured data is from Ref. [3].

for VIV simulations. While the smaller-span models exhibit the same qualitative trend, moderate-to-large differences are observed between them in the *Initial Excitation* and *Upper* branches including underprediction of the peak amplitude.

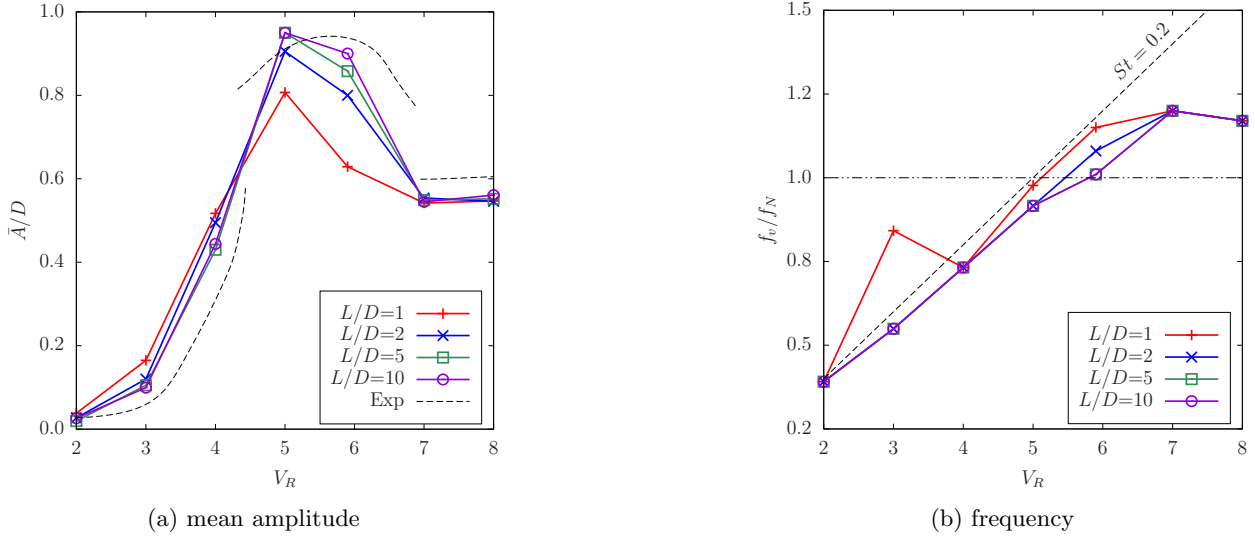


Figure 3: Comparison of predicted (a) \bar{A}/D , and (b) normalized oscillation frequency, using cylinder models of different span lengths.

Peak amplitude is observed at resonance when f_v matches f_N and is expected to occur at $V_R = 1/St$. Since the St at the simulated Re_D is approximately 0.2, peak amplitude occurs at $V_R \sim 5$. Power spectral density (PSD) of the transverse aerodynamic force coefficient, $C_y = 2F_y/(\rho V_\infty^2 L)$ of the four models are compared in Fig. 4 (a) for $V_R = 5$. A linear scale is used to plot the PSDs to accentuate the differences. The spectral peak is higher and narrower for the models with $L \geq 5D$. For shorter-span models, the energy is distributed over a wider frequency range, resulting in a broader peak. A sharp peak in C_y at $k \sim St$ results in greater excitation, hence higher \bar{A}/D , for the larger-span models at $V_R = 5$.

Spanwise coherence of transverse sectional force coefficient, $c_y(z) = 2f_y(z)/(\rho V_\infty^2)$ are plotted in Fig. 4 (b) for $V_R = 5$. For the larger-span cylinders ($L \geq 5D$), high coherence (γ^2) is limited to a very small band of k around St (~ 0.2), whereas for the smaller-span models, γ^2 is very high over the entire span for $0.1 < k < 0.3$. High coherence at frequencies away from $k = St$ is the reason for the broader but shorter peaks observed in the C_y spectra for the smaller-span models.

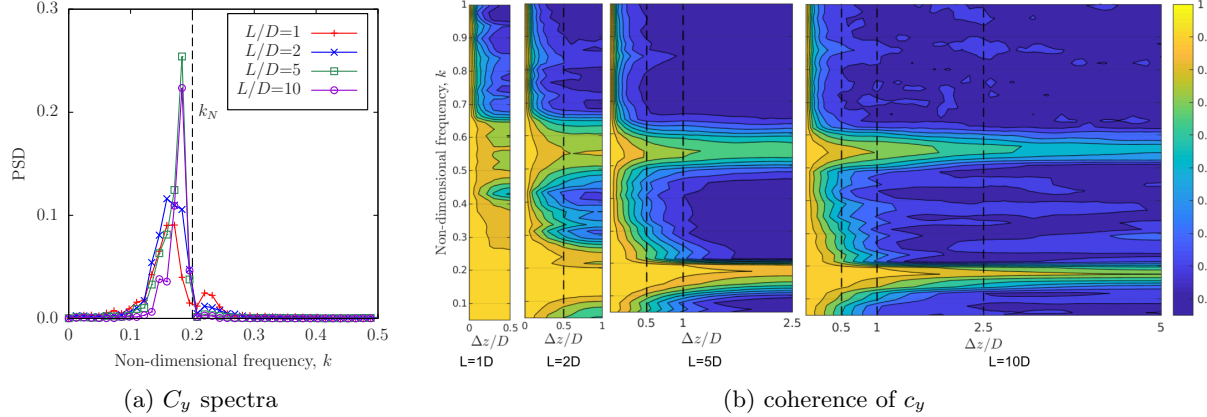


Figure 4: Results at $V_R=5$: (a) PSD of C_y , and (b) $\gamma^2(\Delta z, k)$ of c_y for models with $L/D=1, 2, 5, \& 10$.

Smaller-span models underpredict \bar{A}/D throughout the *Upper* branch. The solutions at $V_R = 5.9$ are probed to investigate this underprediction. Figure 5 plots the C_y spectra and the spanwise coherence of c_y for the different models. The k corresponding to the natural frequency is $k_N = 1/V_R \sim 0.17$ for $V_R = 5.9$. The C_y spectra for the small-span models peak at $k \sim 0.2$ and “lock-in” with k_N does not occur. The spectrum of the largest-span model peaks at around k_N ; the peak is slightly shifted from k_N due to the added-mass effect, which can be substantial for low- m^* systems. High coherence in the small-span models forces the vortex shedding at $k \sim 0.2$ and does not allow “lock-in” at k_N .

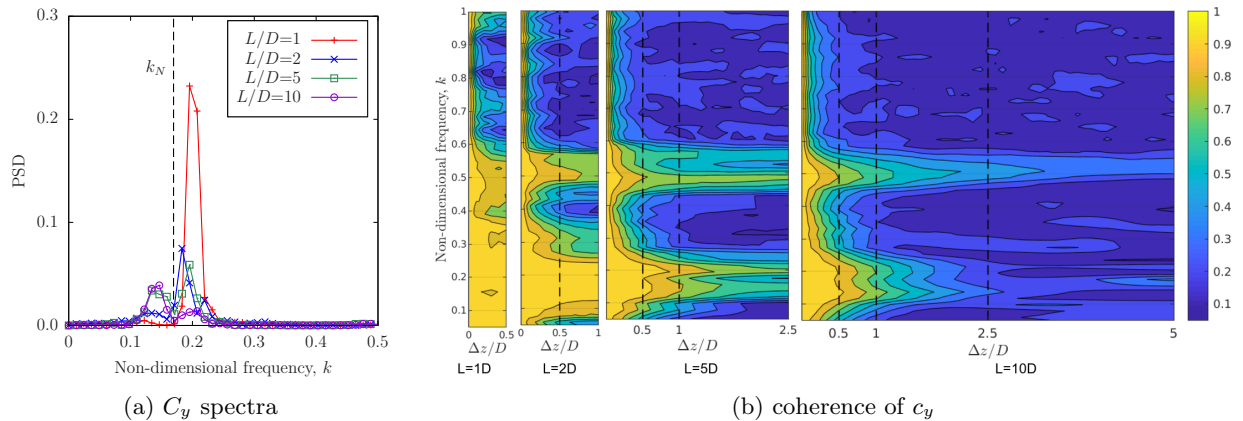


Figure 5: Results at $V_R=5.9$: (a) PSD of C_y , and (b) $\gamma^2(\Delta z, k)$ of c_y for models with $L/D=1, 2, 5, \& 10$.

In contrast to underprediction in the “lock-in” region, the smaller-span models overpredict \bar{A}/D in the *Initial Excitation* branch. This is consistent with the C_y spectra which shows a higher peak at $k \sim 0.2$ for the smaller-span models (see Fig. 6 (a)). Another peak is

observed with the smaller-span models at k near k_N (~ 0.33 for $V_R = 3$). Figure 6 (b) shows increased coherence at k_N . The periodicity in smaller span models reinforces the excitation at this frequency leading to the additional peak in the C_y spectra. In fact, the smallest-span model oscillates at this frequency (see Fig. 3 (b)), suggesting a “lock-in” in the *Initial Excitation* branch.

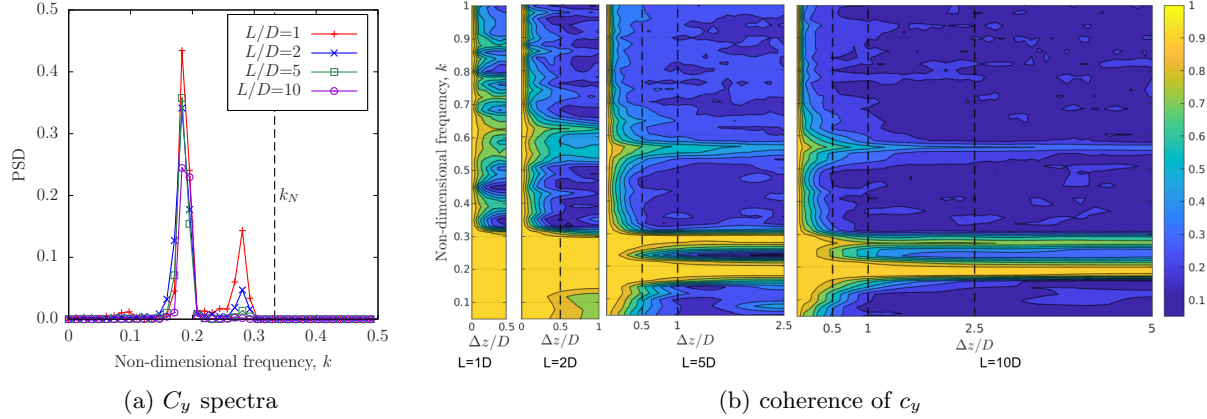


Figure 6: Results at $V_R=3$: (a) PSD of C_y , and (b) $\gamma^2(\Delta z, k)$ of c_y for models with $L/D=1, 2, 5, \& 10$.

4. Conclusion

DES of four finite-span models with periodic span boundaries shows that a minimum span length of $10 D$ is required to accurately simulate VIV. Simulations with smaller-span domains underpredict the peak amplitude of vibration and do not capture the “lock-in” phenomenon accurately. Spanwise coherence of sectional transverse force coefficient provides insights into the observed behavior.

5. Acknowledgments

Funding for this research is provided by the National Science Foundation (Grant #NSF/CMMI-1537917). Computational resources are provided by NSF XSEDE (Grant #TG-CTS130004) and the Argonne Leadership Computing Facility, which is a DOE Office of Science User Facility supported under Contract DE-AC02-06CH11357.

References

1. Yin, Z., Reddy, K., Durbin, P.A.. On the dynamic computation of the model constant in delayed detached eddy simulation. *Physics of Fluids* 2015;**27**(2).
2. Wu, X., Jafari, M., Sarkar, P., Sharma, A.. Verification of des for flow over rigidly and elastically-mounted circular cylinders in normal and yawed flow. *Journal of Fluids and Structures* 2019;.
3. Khalak, A., Williamson, C.. Fluid forces and dynamics of a hydroelastic structure with very low mass and damping. *Journal of Fluids and Structures* 1997;**11**(8):973–982.